Regulation of prelamin A but not lamin C by miR-9, a brain-specific microRNA

Hea-Jin Jung[a], Catherine Coffinier[b], Youngshik Choe[c], Anne P. Beigneux[b], Brandon S. J. Davies[b], Shao H. Yang[b], Richard H. Barnes II[b], Janet Hong[d], Tao Sun[d], Samuel J. Pleasure[c], Stephen G. Young[a,b,e,1], and Loren G. Fong[b,1]

[a]Molecular Biology Institute and Departments of [b]Medicine and [e]Human Genetics, University of California, Los Angeles, CA 90095; [c]Department of Neurology, University of California, San Francisco, CA 94158; and [d]Department of Cell and Developmental Biology, Weill Medical College of Cornell University, New York, NY 10065

Edited by Jonathan G. Seidman, Harvard Medical School, Boston, MA, and approved December 27, 2011 (received for review July 20, 2011)

Lamins A and C, alternatively spliced products of the *LMNA* gene, are key components of the nuclear lamina. The two isoforms are found in similar amounts in most tissues, but we observed an unexpected pattern of expression in the brain. Western blot and immunohistochemistry studies showed that lamin C is abundant in the mouse brain, whereas lamin A and its precursor prelamin A are restricted to endothelial cells and meningeal cells and are absent in neurons and glia. Prelamin A transcript levels were low in the brain, but this finding could not be explained by alternative splicing. In lamin A-only knockin mice, where alternative splicing is absent and all the output of the gene is channeled into prelamin A transcripts, large amounts of lamin A were found in peripheral tissues, but there was very little lamin A in the brain. Also, in knockin mice expressing exclusively progerin (a toxic form of prelamin A found in Hutchinson–Gilford progeria syndrome), the levels of progerin in the brain were extremely low. Further studies showed that prelamin A expression, but not lamin C expression, is down-regulated by a brain-specific microRNA, miR-9. Expression of miR-9 in cultured cells reduced lamin A expression, and this effect was abolished when the miR-9–binding site in the prelamin A 3′ UTR was mutated. The down-regulation of prelamin A expression in the brain could explain why mouse models of Hutchinson–Gilford progeria syndrome are free of central nervous system pathology.

genetic diseases | A-type lamins | nucleus | differential gene expression | silencing

The nuclear lamina, an intermediate filament meshwork located adjacent to the inner nuclear membrane, provides scaffolding for the cell nucleus and plays a role in many vital processes in the cell, including the regulation of gene expression and chromatin structure (1, 2). The nuclear lamina is composed primarily of four lamin proteins: lamins A, B1, B2, and C (3). Lamins B1 and B2, generally referred to as the "B-type lamins," are products of independent genes (*LMNB1* and *LMNB2,* respectively). Lamins A and C, called the "A-type lamins," are alternatively spliced products of the same gene, *LMNA*, and are found in roughly similar amounts in most tissues (4). The lamin C transcript contains exon 1–10 sequences, whereas the transcript for prelamin A (the precursor to lamin A) contains exon 1–12 sequences; the 3′ UTRs of the two transcripts are distinct.

Prelamin A, but not lamin C, terminates with a *CaaX* motif and undergoes farnesylation of the carboxyl-terminal cysteine (the "*C*" of the *CaaX* motif). Following protein farnesylation, prelamin A undergoes three additional processing steps: endoproteolytic release of the last three amino acids of the protein (i.e., the *–aaX*), methylation of the newly exposed farnesylcysteine, and a second endoproteolytic cleavage event, mediated by ZMPSTE24, that releases 15 additional amino acids from the carboxyl terminus, including the farnesylcysteine methyl ester (5, 6). The last cleavage step releases mature lamin A.

Lamins A and C have attracted considerable interest with the discovery that mutations in *LMNA* cause multiple human diseases (5). Missense mutations involving residues common to lamins A and C have been shown to cause muscular dystrophy, cardiomyopathy, and lipodystrophy (5). However, a few mutations, for example those causing Hutchinson–Gilford progeria syndrome (HGPS), alter the structure of prelamin A without affecting lamin C (7, 8). In HGPS, single-nucleotide mutations lead to aberrant mRNA splicing, resulting in the synthesis of a mutant prelamin A, generally called "progerin," that has an in-frame deletion of 50 amino acids. That deletion does not affect the farnesylation or methylation of the carboxyl terminus but abolishes the final step in lamin A biogenesis; hence, progerin retains a farnesylcysteine methyl ester at its carboxyl terminus. Progerin is toxic to cells and elicits pathology in multiple tissues, resulting in phenotypes resembling physiologic aging (e.g., atherosclerosis, alopecia, and osteoporosis) (9). However, some phenotypes commonly associated with aging, for example senile dementia, are absent. Several years ago, Yang et al. (10) generated a knockin mouse model that produces high levels of progerin ($Lmna^{HG/+}$ mice); these mice develop many progeria-like disease phenotypes; however, the central nervous system is free of disease.

We sought to understand why knockin mice that synthesize a toxic protein, namely progerin, might be spared from central nervous system pathology. One potential explanation would be that the brain, in contrast to other tissues, synthesizes mainly lamin C and little prelamin A. In the current study, we tested that possibility and in the process uncovered a mechanism for the regulation of prelamin A expression.

Results

We began by using Western blots to examine lamin A and lamin C expression in different tissues of wild-type mice ($Lmna^{+/+}$) (Fig. 1*A*). Consistent with earlier studies (4, 11, 12), large amounts of both lamin A and lamin C were found in the liver, heart, and kidney, with the lamin A band being slightly more intense than the lamin C band (Fig. 1*A*). In contrast, the cerebellum and cerebral cortex expressed mainly lamin C and far less lamin A (Fig. 1*A*). Neither lamin A nor lamin C was expressed in tissues of $Lmna^{-/-}$ mice (13).

The preferential expression of lamin C in the brain was supported further by Western blots of tissue extracts from $Zmpste24^{-/-}$ mice (Fig. 1*B*). ZMPSTE24 deficiency abolishes the production of mature lamin A and leads to the accumulation of a farnesylated form of prelamin A in cells (14, 15). We observed

Author contributions: H.-J.J., C.C., S.G.Y., and L.G.F. designed research; H.-J.J., Y.C., A.P.B., B.S.J.D., S.H.Y., R.H.B., J.H., and L.G.F. performed research; H.-J.J. contributed new reagents/analytic tools; H.-J.J., C.C., T.S., S.J.P., S.G.Y., and L.G.F. analyzed data; and H.-J.J., S.G.Y., and L.G.F. wrote the paper.

The authors declare no conflict of interest.

This article is a PNAS Direct Submission.

[1]To whom correspondence may be addressed. E-mail: lfong@mednet.ucla.edu or sgyoung@mednet.ucla.edu.

See Author Summary on page 2204.

This article contains supporting information online at www.pnas.org/lookup/suppl/doi:10.1073/pnas.1111780109/-/DCSupplemental.

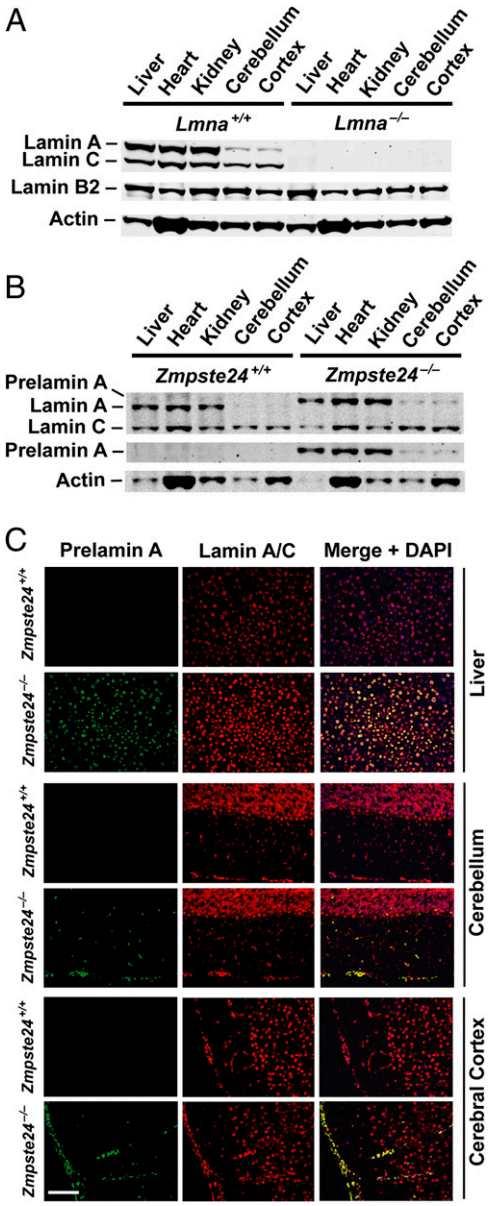

Fig. 1. Distinct expression patterns of lamins A and C in the mouse brain. (*A*) Western blot of tissue extracts from *Lmna*$^{+/+}$ (wild-type) and *Lmna*$^{-/-}$ mice with antibodies against lamin A/C, lamin B2, and actin. (*B*) Western blot of tissue extracts from *Zmpste24*$^{+/+}$ and *Zmpste24*$^{-/-}$ mice (14) with antibodies against lamin A/C, prelamin A, and actin. (*C*) Immunofluorescence microscopy images of tissues from wild-type (*Zmpste24*$^{+/+}$) and *Zmpste24*$^{-/-}$ mice. Frozen sections of liver, cerebellum, and cerebral cortex were stained with antibodies against prelamin A (green) and lamin A/C (red); DNA was stained with DAPI. Prelamin A was undetectable in *Zmpste24*$^{+/+}$ mice. Prelamin A was present in the brain of *Zmpste24*$^{-/-}$ mice but only in scattered cells within the parenchyma of the brain and meningeal cells. (Scale bar, 100 μm.)

substantial amounts of prelamin A in the peripheral tissues of *Zmpste24*$^{-/-}$ mice, but far less prelamin A was detected in the cerebellum and cerebral cortex (Fig. 1*B*).

The low levels of prelamin A expression in the brain of *Zmpste24*$^{-/-}$ mice were obvious by immunohistochemistry (Fig. 1*C*). In the tissues of wild-type mice (*Zmpste24*$^{+/+}$), staining for prelamin A was virtually undetectable, reflecting the fact that prelamin A is converted efficiently to mature lamin A (Fig. 1*C*) (16). In the liver of *Zmpste24*$^{-/-}$ mice, prelamin A accumulates; hence cell nuclei were stained with both a prelamin A-specific antibody and a lamin A/C antibody. In the brain, however, the staining patterns for the two antibodies were different; the lamin A/C antibody bound to the nuclei of all cells, but staining with the prelamin A antibody was restricted to scattered cells in the parenchyma of the brain and meningeal cells on the surface of the brain.

Similar immunohistochemical findings were observed in tissues of wild-type mice stained with antibodies against lamin A, lamin C, and lamin B2 (Fig. S1). In the liver of wild-type mice, cell nuclei were stained with both lamin A- and lamin C-specific antibodies. In the brain, nearly all cells were stained by the lamin C antibody, but only cells along the surface of the brain and scattered cells within the brain were stained positively with the lamin A antibody (Fig. S1). As expected, neither lamin A nor lamin C was detected in *Lmna*$^{-/-}$ mouse tissues, and lamin B2 was expressed by all cells in both wild-type and *Lmna*$^{-/-}$ mice (Fig. S1).

We suspected that most prelamin A- and lamin A-positive cells within the brain parenchyma (Fig. 1*C* and Fig. S1) were vascular endothelial cells. To examine this notion, a fluorescently labeled tomato lectin (17) was injected i.v. into wild-type mice to stain endothelial cells, and the tissues then were examined by immunohistochemistry (Fig. 2*A* and Fig. S2). Again, we found ubiquitous expression of lamin C in the brain, whereas lamin A expression was restricted to meningeal cells along the surface of the brain and cells associated with lectin-stained blood vessels. Staining of the brain with an antibody against CD31 (a marker of endothelial cells) confirmed that most lamin A-expressing cells in the brain are vascular cells (Fig. 2*B*).

To characterize lamin A-expressing cells in the brain further, we stained brain sections from wild-type mice with an antibody against lamin A in combination with an antibody against lamin C, GFAP, Olig2, Zic2, or NeuN (Fig. S3). The antibodies against GFAP and a transcription factor, Olig2, identified astrocytes and oligodendrocytes, respectively; an antibody against NeuN was used as a neuronal marker, and an antibody against Zic2 served as a marker for Purkinje cells. We observed lamin C expression throughout the brain, including Purkinje cells and granular cells of the cerebellum (Fig. S3 *A* and *C*, *Top*). In contrast, lamin A was not found in Zic2^{+} Purkinje cells in the cerebellum or Olig2^{+} oligodendrocytes in the cerebellum and hippocampus (Fig. S3 *A* and *B*). Most regions of the brain that were stained positively for GFAP were devoid of lamin A (Fig. S3 *A* and *B*). NeuN^{+} cells in the granular layer of the cerebellum were stained positively for lamin C but not lamin A (Fig. S3*C*). These observations, combined with the lectin/CD31 immunohistochemistry studies (Fig. 2 and Fig. S2), suggest that most cells in the brain express lamin C but that lamin A is restricted mainly to vascular and meningeal cells.

Cultured neurons also preferentially express lamin C. We isolated neural progenitor cells (NPCs) from the cortex of E13.5 wild-type mouse embryos and allowed them to differentiate in culture. By Western blot, a prominent lamin C band was detected after 12 d of culture, but the lamin A band was faint (Fig. S4*A*). Immunocytochemistry with antibodies against lamin A, lamin C, and β3 tubulin (a neuron-specific tubulin) supported the idea that neurons express primarily lamin C. Cell nuclei that were surrounded by β3 tubulin (TU-20)-positive cytoplasm were positive for lamin C but not lamin A (Fig. S4 *B–D*), whereas lamin A-expressing cells were negative for β3 tubulin (Fig. S4 *B–D*).

The preferential expression of lamin C protein in the brain prompted us to examine the expression of prelamin A and lamin C transcripts. We began with Northern blots using a probe common to prelamin A and lamin C transcripts (Fig. 3*A*). In the kidney of wild-type mice, the intensities of the prelamin A and lamin C bands were similar. The intensities of the lamin C bands in the brain were similar to those in the kidney, but the prelamin A bands were faint. We also examined transcripts in two *Lmna* knockin mice—

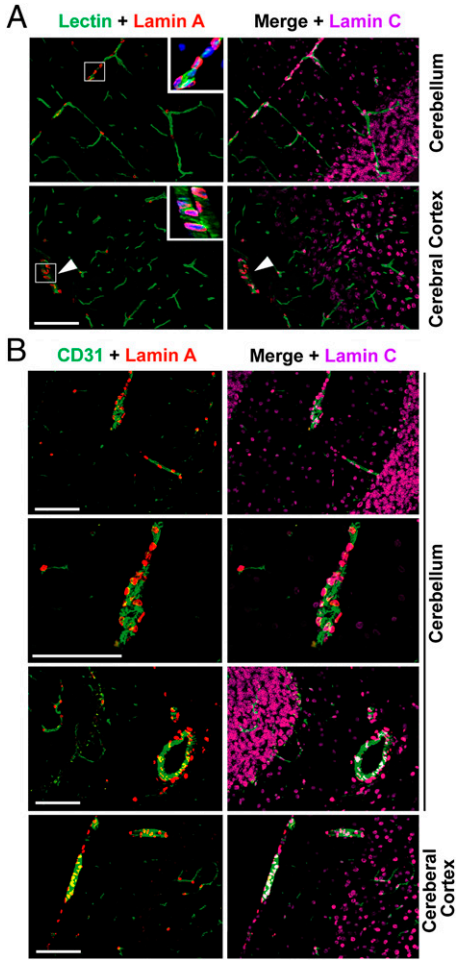

Fig. 2. Cells expressing lamin A in the mouse brain are located predominantly in blood vessels and meninges. (*A*) FITC-labeled tomato lectin (17) (green) was injected i.v. into wild-type mice to stain blood vessels. Frozen sections of the brain were stained for lamin A (red) and lamin C (magenta). Lamin C was found in most cells in the brain, but lamin A was found mainly in association with capillaries or meningeal cells lining the surface of the brain (arrowhead). (Scale bar, 100 μm.) *Insets* show high-magnification views of lamin A expression in lectin-positive blood vessels. Nuclei were stained with DAPI (blue). (*B*) Frozen sections of the brain from wild-type mice were stained with antibodies against lamin A (red), lamin C (magenta), and CD31 (green). Most lamin A–positive cells were found in association with CD31, a marker of endothelial cells. (Scale bars, 100 μm.)

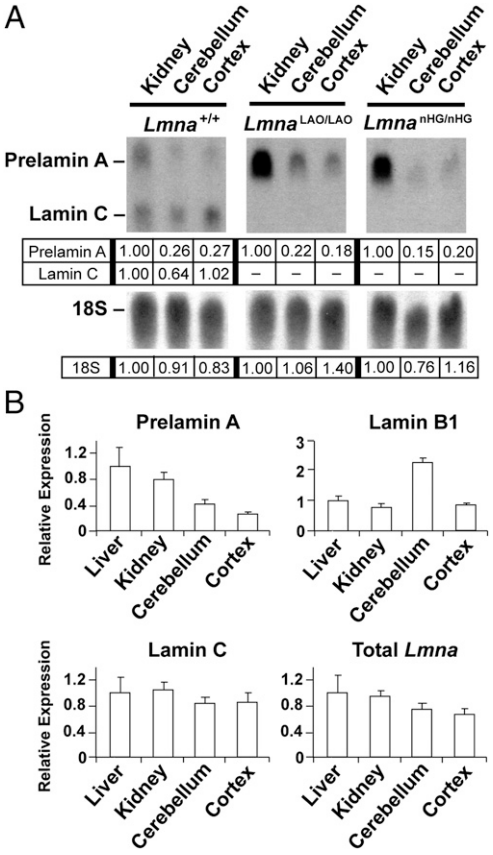

Fig. 3. Preferential expression of lamin C transcripts in the mouse brain. (*A*) Northern blot of total RNA from *Lmna*$^{+/+}$, *Lmna*$^{LAO/LAO}$, and *Lmna*$^{nHG/nHG}$ mice with a ^{32}P-labeled probe made from cDNA sequences shared by prelamin A and lamin C transcripts. An 18S rRNA probe was used as a loading control. Signals were quantified with ImageJ software, and values were normalized to those in the kidney (set at a value of 1.0). (*B*) qRT-PCR analysis of prelamin A, lamin B1, lamin C, and total *Lmna* transcripts in wild-type mouse tissues. Data were normalized to cyclophilin A, and gene expression was compared with that in the liver (which was set at 1.0). Values represent mean ± SD from four different wild-type mice.

Lmna$^{LAO/LAO}$ mice that express exclusively mutant prelamin A transcripts encoding mature lamin A (18) and *Lmna*$^{nHG/nHG}$ mice that express mutant prelamin A transcripts encoding non-farnesylated progerin (*Materials and Methods*) (12). Lamin C transcripts were absent, as expected, in both knockin models, but, similar to wild-type mice, the levels of prelamin A transcripts were much lower in the brain than in the kidney (Fig. 3*A*).

We performed quantitative RT-PCR (qRT-PCR) on RNA from tissues of wild-type mice to quantify (*i*) prelamin A transcripts, using primers unique to prelamin A; (*ii*) lamin C transcripts, using primers unique to lamin C; (*iii*) lamin B1 transcripts; and (*iv*) total *Lmna* transcripts, using primers that bind to sequences common to prelamin A and lamin C (Fig. 3*B*). Expression levels were normalized to cyclophilin A and compared with those in the liver (set as 1.0). Consistent with the Northern blots, the levels of lamin C transcripts in the cerebellum and cerebral cortex were nearly (~85%) as high as those in the peripheral tissues (Fig. 3*B*). In contrast, the levels of prelamin A transcripts in the cerebellum and cortex were only 25–40% of those in the liver. Consistent with those results, total *Lmna* transcripts were ~65–75% as high as those in the liver.

The preferential expression of lamin C in the brain was confirmed by in situ hybridization. In the brain of a wild-type mouse, *Lmna* expression was detected easily with a riboprobe common to prelamin A and lamin C, but not with a prelamin A-specific probe (Fig. S5). As expected, no hybridization signal was detected in the brain of an *Lmna*$^{-/-}$ mouse (Fig. S5).

We initially suspected that alternative mRNA splicing would explain the preferential expression of lamin C in the brain. To test this idea, we examined lamin A expression in *Lmna*$^{LAO/LAO}$ mice in which all the output of the *Lmna* gene is channeled into the production of mutant prelamin A transcripts encoding mature lamin A (18). Because lamin C splicing is absent in these mice, we expected to find increased levels of lamin A in the brain (i.e., levels comparable to lamin C levels in the brain of wild-type mice). To our surprise, Western blots revealed very low levels of lamin A in the cerebellum and cortex (Fig. 4*A*), consistent with our Northern blot findings (Fig. 3*A*). Furthermore, by immunohistochemistry, lamin A was nearly absent in the brain of *Lmna*$^{LAO/LAO}$ mice, except in vascular structures and meningeal cells (Fig. 4*B*). Thus, even though all the output of the *Lmna*^{LAO} allele was channeled into production of prelamin A transcripts,

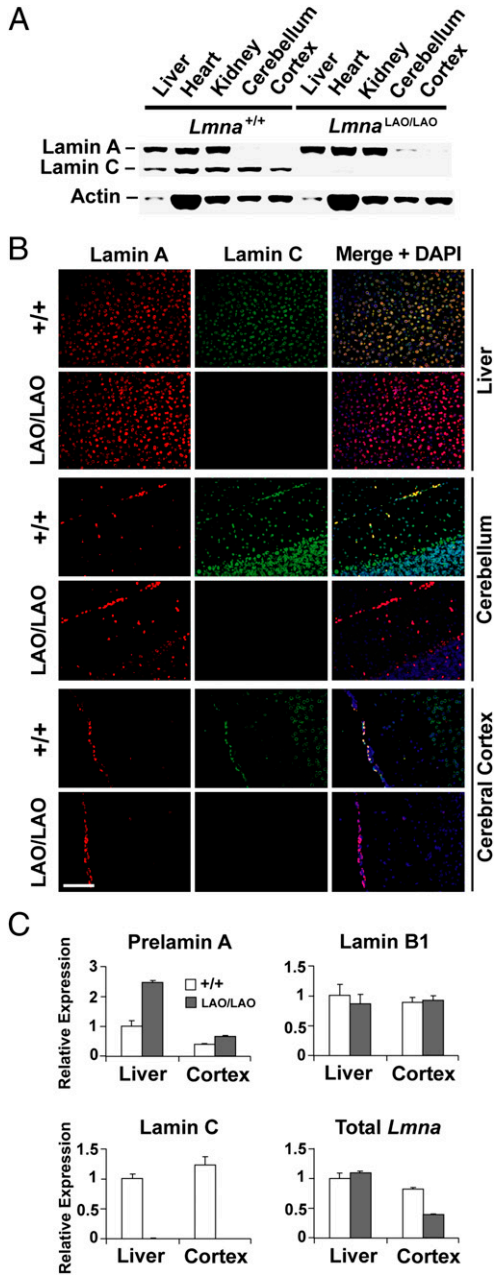

Fig. 4. Low expression levels of lamin A in the brain of *Lmna*$^{LAO/LAO}$ mice, in which all the output of the *Lmna* gene is channeled into the production of prelamin A transcripts (18). (*A*) Western blot of tissue extracts from *Lmna*$^{+/+}$ and *Lmna*$^{LAO/LAO}$ mice with antibodies against lamin A/C and actin. (*B*) Immunofluorescence microscopy of the liver, cerebellum, and cerebral cortex from *Lmna*$^{+/+}$ and *Lmna*$^{LAO/LAO}$ mice. Sections were stained with antibodies against lamin A (red) and lamin C (green), and nuclei were visualized with DAPI. The lamin A expression pattern in the brain of *Lmna*$^{LAO/LAO}$ mice was virtually identical to that in wild-type mice (Figs. 1 and 2), with scattered lamin A-positive vascular cells. (Scale bar, 100 μm.) (*C*) qRT-PCR analysis of prelamin A, lamin B1, lamin C, and total *Lmna* transcripts in the liver and cortex of *Lmna*$^{+/+}$ and *Lmna*$^{LAO/LAO}$ mice. Data were normalized to cyclophilin A, and gene expression was compared with that of the wild-type liver (which was set at 1.0). Values represent mean ± SD from three pairs of mice.

the levels of lamin A in the brain of *Lmna*$^{LAO/LAO}$ mice were low, similar to the situation in wild-type mice (Fig. 4 *A* and *B*).

The low levels of lamin A in the brain of *Lmna*$^{LAO/LAO}$ mice, as judged by both Western blots and immunohistochemistry, prompted us to investigate further the *Lmna* transcript levels in those mice (Fig. 4*C*). In the liver of *Lmna*$^{LAO/LAO}$ mice, the total *Lmna* transcript levels were virtually identical to those in wild-type mice (i.e., the absence of lamin C expression was offset by twice-normal expression of prelamin A). In the cerebral cortex, however, total *Lmna* transcript levels were much lower than those in wild-type mice (Fig. 4*C*).

We also examined the expression of progerin in the brain of mice harboring an *Lmna*^{nHG} allele (which yields prelamin A transcripts encoding nonfarnesylated progerin but no lamin C transcripts) (12). Again, lamin A and progerin levels were quite low in the cerebellum and cerebral cortex of *Lmna*$^{nHG/+}$ and *Lmna*$^{nHG/nHG}$ mice (Fig. 5), in keeping with findings in wild-type (Fig. 1*A*), *Zmpste24*$^{-/-}$ (Fig. 1*B*), and *Lmna*$^{LAO/LAO}$ mice (Fig. 4*A*).

We considered the possibility that the low levels of prelamin A transcripts in the brain might be caused by low transcription rates. To address this possibility, we measured heterogeneous nuclear RNA (hnRNA) levels (i.e., pre-mRNA levels) for prelamin A in the brain and liver of wild-type and *Lmna*$^{LAO/LAO}$ mice. Interestingly, prelamin A hnRNA levels were higher in the brain than in the liver (Fig. S6 *A* and *B*), weighing against the possibility of reduced prelamin A transcription in the brain. Also, we considered the possibility that the low levels of prelamin A transcripts in the brain somehow might relate to the use of a different *Lmna* promoter in the brain. However, 5′-RACE experiments did not support this idea; the 5′ UTR of *Lmna* transcripts in the brain was identical to that in other tissues (Fig. S6*C*).

The low levels of lamin A in the brain of *Lmna*$^{LAO/LAO}$ mice and the low levels of progerin in the brain of *Lmna*$^{nHG/nHG}$ mice led us to suspect that the brain must have a mechanism other than alternative splicing for reducing prelamin A expression, and we hypothesized that this mechanism might involve the prelamin A 3′ UTR. The prelamin A 3′ UTR contains sequences that are predicted by miRanda (http://www.microrna.org/microrna/home.do) to be binding sites for two brain-specific microRNAs—one for miR-9 (site 2 in Fig. 6*A*) and one for miR-129. In addition, by scanning the 3′ UTR sequences, we identified another potential miR-9–binding site in the prelamin A 3′ UTR (site 1 in Fig. 6*A*). We also identified a potential miR-9–binding site in the lamin C 3′ UTR (C-site 1 in Fig. 6*A*).

To assess the relevance of miR-9 and miR-129 in regulating lamin A/C expression, miR-9 or miR-129 expression vectors were transfected into HeLa cells (which do not express either microRNA), and cells were subjected to selection with puromycin. HeLa cells transfected with miR-9 expressed high levels of miR-9, but these levels were lower than those in the cerebral cortex of 1-mo-old mice (Fig. S7). Transfection of the miR-129 vector yielded miR-129 levels that were higher than those in the cerebral cortex of 1-mo-old mice (Fig. S7). As judged by Western blots, lamin A levels in miR-9–expressing cells fell by ~50% relative to lamin C, but there were no significant changes in lamin A levels in miR-129–transfected cells (Fig. 6 *B* and *C*).

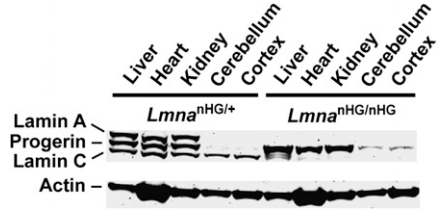

Fig. 5. Western blot analysis of lamin A, lamin C, and progerin expression in tissues of *Lmna*$^{nHG/+}$ and *Lmna*$^{nHG/nHG}$ mice with antibodies against lamin A/C and actin.

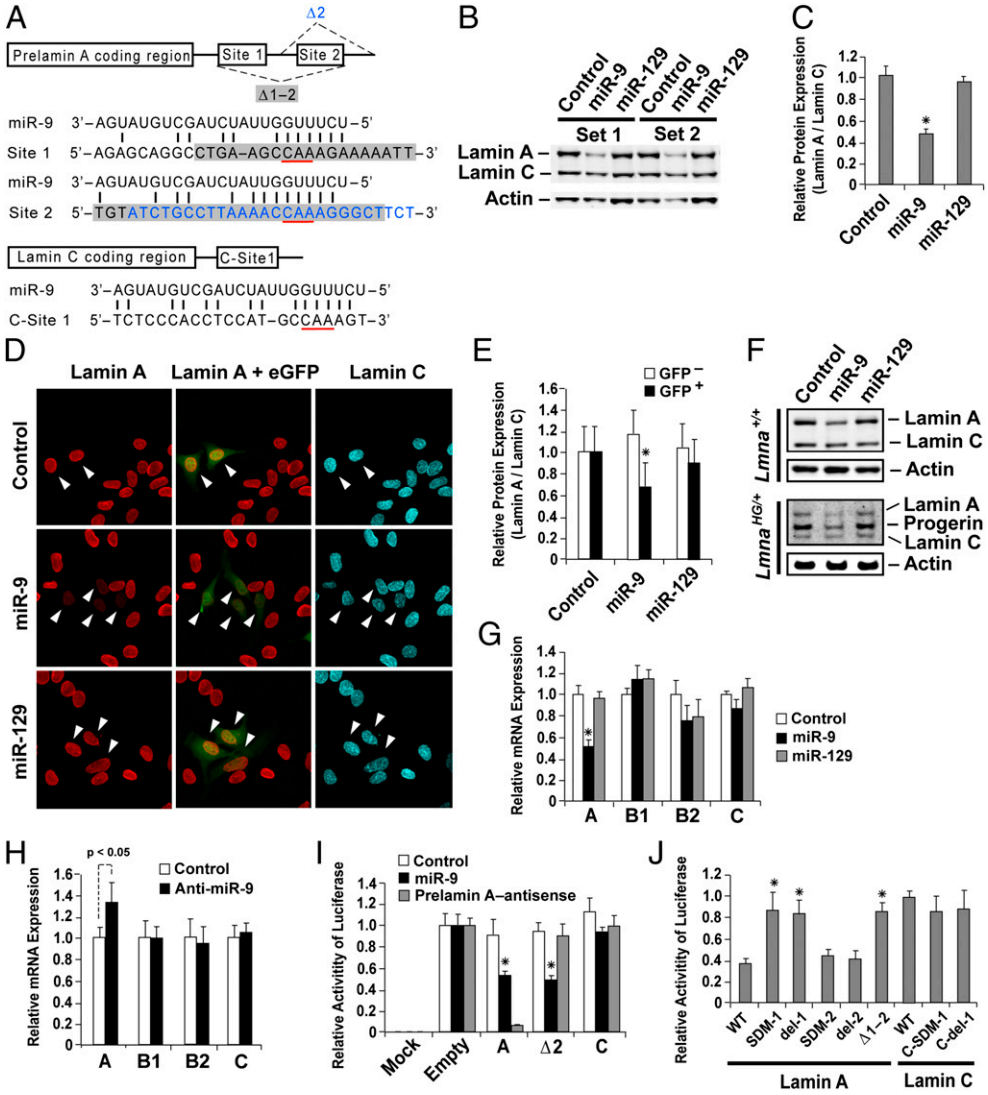

Fig. 6. Down-regulation of lamin A expression by miR-9. (*A*) Predicted miR-9–binding sites in the 3′ UTR of prelamin A and lamin C. The regions that were truncated in luciferase reporter vectors (Δ2 and Δ1–2; see *I* and *J*) are shown, and the exact sequences are indicated by blue font (Δ2) or highlighted in gray (Δ1–2). The three nucleotides that were mutated or deleted in other mutant constructs (SDM-1, del-1, SDM-2, del-2, C-SDM-1, and C-del-1; *J*) are underlined in red. (*B*) Western blot analysis of lamin A and C expression in HeLa cells 3.5 d after transfection with an empty vector, an miR-9 expression vector, or an miR-129 expression vector. All cells had been subjected to puromycin selection. Shown are representative data from two independent experiments (set 1 and set 2). (*C*) Quantification of the lamin A signals in the Western blots (normalized to lamin C levels). Results show mean ± SD from four independent experiments. (*D*) Immunofluorescence microscopy to assess lamin A and C expression in HeLa cells that had been transiently transfected with miR-9 or miR-129 expression vectors (or an empty vector). Transfected cells were identified by EGFP expression (arrowheads). (*E*) Quantification of the immunofluorescence signals from the immunofluorescence microscopy experiments. The lamin A signals were normalized to lamin C. Values represent mean ± SD (from examining ≥146 cells per condition). (*F*) Western blot studies of immortalized *Lmna*$^{+/+}$ and *Lmna*$^{HG/+}$ fibroblasts transduced with lentiviruses encoding miR-9 or miR-129 (or an empty vector). All cells had been subjected to puromycin selection. (*G*) qRT-PCR analysis of prelamin A, lamin B1, lamin B2, and lamin C transcript levels in HeLa cells transfected with miR-9 or miR-129 expression vectors (or an empty vector). All cells had been subjected to puromycin selection. Data were normalized to cyclophilin A, and gene expression was compared with that of empty vector-transfected cells (set at 1.0). Values represent mean ± SD from four independent experiments. (*H*) qRT-PCR analysis of prelamin A, lamin B1, lamin B2, and lamin C expression levels in differentiated NPCs transfected with an miR-9 antisense oligonucleotide or a control antisense oligonucleotide. Data were normalized to cyclophilin A, and gene expression in the miR-9 antisense-transfected cells was compared with that of cells transfected with the control oligonucleotides (set at 1.0). Values represent mean ± SD from three independent experiments. (*I*) Luciferase assays in HeLa cells that had been cotransfected with an empty vector or an miR-9 expression vector along with luciferase plasmids harboring the prelamin A 3′ UTR, a truncated version of the prelamin A 3′ UTR (Δ2; see schematic in *A*), or the lamin C 3′ UTR. After 30 h, firefly luciferase activities were measured, normalized to levels of Renilla luciferase activities, and compared with those of empty luciferase vector (pmirGLO)–transfected cells (set at 1.0). An antisense oligonucleotide against prelamin A was used as a control. Values represent mean ± SD from three independent experiments. (*J*) Luciferase assays with luciferase reporter vectors in which the miR-9 seed-binding sequence (CCAAAG) in the 3′ UTR of prelamin A and lamin C was mutated. From left to right: WT, wild-type 3′ UTR of prelamin A; SDM-1, substitution of the three nucleotides in site 1 of the prelamin A 3′ UTR (CAA) with ACC; del-1, deletion of the CAA in site 1 of the prelamin A 3′ UTR; SDM-2, replacement of the CAA in site 2 of the prelamin A 3′ UTR by ACC; del-2, deletion of the CAA in site 2 of the prelamin A 3′ UTR; Δ1–2, an internal truncation encompassing both sites 1 and 2 of the prelamin A 3′ UTR; WT, wild-type 3′ UTR of lamin C; C-SDM-1, replacement of CAA by ACC in site 1 of the lamin C 3′ UTR; C-del-1, deletion of the CAA in site 1 of the lamin C 3′ UTR. After 24 h, firefly luciferase activities were measured, normalized to levels of Renilla luciferase activities, and compared with those from the cells transfected with the luciferase vector containing the wild-type 3′ UTR of lamin C (set at 1.0). Values represent mean ± SD from three independent experiments. *$P < 0.0001$.

We also used immunocytochemistry to assess the effects of miR-9 on the expression of lamin A, lamin C, and lamin B1 in transiently transfected cells (transfected cells could be identified because the microRNA expression vectors also produced EGFP) (Fig. 6 *D* and *E* and Fig. S8). Fluorescence microscopy revealed that miR-9, but not miR-129, reduced lamin A expression in transfected HeLa cells (Fig. 6*D* and Fig. S8). Neither miR-9 nor miR-129 affected lamin C expression (Fig. 6*D*). Quantification of the fluorescent signals with Volocity software (Perkin-Elmer) indicated that lamin A expression was reduced by ~40% in miR-9–transfected cells, relative to lamin C (Fig. 6*E*) or lamin B1 (Fig. S8).

The effects of miR-9 on lamin A expression also were examined in immortalized mouse embryonic fibroblasts (MEFs) (Fig. 6*F*). Wild-type MEFs and MEFs heterozygous for a progerin-only knockin allele ($Lmna^{HG/+}$) were transduced with lentiviruses encoding miR-9 or miR-129 and subjected to puromycin selection. The expression of miR-9, but not miR-129, lowered lamin A levels (relative to lamin C) in $Lmna^{+/+}$ cells, as judged by Western blots (Fig. 6*F*). In $Lmna^{HG/+}$ cells, miR-9 reduced levels of lamin A and progerin, but not lamin C (Fig. 6*F*).

We used qRT-PCR to quantify the effects of miR-9 expression on transcript levels of different nuclear lamins in HeLa cells (Fig. 6*G*). These studies showed that miR-9 expression reduced the levels of prelamin A transcripts but not those of the other lamins (Fig. 6*G*). We also tested whether suppressing endogenous miR-9 expression in differentiated neural progenitor cells would affect prelamin A transcript levels. Neural progenitor cells isolated from embryonic day 13.5 (E13.5) cortical explants were cultured in differentiation medium for 13 d and then transfected with an antisense oligonucleotide against miR-9 or a control oligonucleotide (with no homology to miR-9). When the cells were transfected with the miR-9 antisense oligonucleotide, miR-9 levels fell to almost undetectable levels, and prelamin A transcript levels increased by ~25% (Fig. 6*H*).

We suspected that the effects of miR-9 on prelamin A transcript levels were mediated by direct binding of miR-9 to the prelamin A 3′ UTR. To test this possibility, HeLa cells were transfected with an miR-9 expression vector (or an empty vector) along with luciferase reporter vectors containing a wild-type version of the prelamin A 3′ UTR or a truncated version of the prelamin A 3′ UTR (Δ2, containing site 1 but not site 2; see schematic in Fig. 6*A*) or the lamin C 3′ UTR. As a control, we transfected cells with an antisense oligonucleotide against the prelamin A 3′ UTR (19). MiR-9 overexpression lowered luciferase expression from the luciferase reporter vector containing the entire prelamin A 3′ UTR but not from the vector containing the lamin C 3′ UTR (Fig. 6*I*). Interestingly, miR-9 also reduced luciferase expression with the vector lacking site 2 in the prelamin A 3′ UTR (Δ2, Fig. 6*I*), suggesting that the effects of miR-9 were mediated by site 1 in the prelamin A 3′ UTR. As expected, the effects of the antisense oligonucleotide on luciferase expression were not observed with the Δ2 mutant (Fig. 6*I*), which lacks the sequence complementary to the antisense oligonucleotide (downstream of site 2 in the prelamin A 3′ UTR).

To determine if site 1 in the prelamin A 3′ UTR mediates the effects of miR-9 on prelamin A transcript levels, we generated luciferase reporter vectors in which the miR-9 seed-binding sequence (CCAAAG) in site 1 or site 2 was mutated. The mutations included (*i*) replacing the three nucleotides of site 1 (CAA) with ACC (SDM-1); (*ii*) deleting the CAA in site 1 (del-1); (*iii*) replacing the CAA in site 2 with ACC (SDM-2); (*iv*) deleting the CAA in site 2 (del-2); and (*v*) a truncation encompassing both sites 1 and 2 (Δ1–2) (see schematic in Fig. 6*A*). The putative miR-9 seed-binding sequence in the lamin C 3′ UTR also was examined with two mutations: (*i*) substitution of the CAA with ACC (C-SDM-1) and (*ii*) deletion of the CAA (C-del-1) (see schematic in Fig. 6*A*). Luciferase reporter studies with the new vectors supported the notion that site 1 is crucial (Fig. 6*J*). MiR-9 expression reduced luciferase expression from the vector containing the wild-type prelamin A 3′ UTR, but when the CAA in site 1 was mutated or deleted (SDM-1, del-1, Δ1–2), the effect of miR-9 on luciferase expression was abolished (Fig. 6*J*). In contrast, when the CAA in the prelamin A site 2 was mutated or deleted (SDM-2, del-2), miR-9 expression remained effective in lowering luciferase expression, similar to results with the wild-type version of the prelamin A 3′ UTR. Mutation or deletion of the CAA in the lamin C 3′ UTR (C-SDM-1, C-del-1) had no effect on luciferase expression levels (Fig. 6*J*).

To confirm the specificity of the regulation of prelamin A by miR-9, we generated a mutant version of miR-9 expression vector by replacing TTG in the miR-9 seed sequence (CTTTGG) with GGT. When the mutant miR-9 expression vector was tested in luciferase-prelamin A 3′ UTR experiments (identical to those shown in Fig. 6*J*), we found no effect of the mutant miR-9 vector on the expression of luciferase-prelamin A 3′ UTR constructs (Fig. S9*A*). In contrast, the wild-type miR-9 expression vector lowered luciferase expression (Fig. S9*A*), as it did in the experiments in Fig. 6*J*.

We also examined the impact of the mutant miR-9 expression vector on prelamin A transcripts in HeLa cells, and we found that it had no effect (Fig. S9*B*). In addition to prelamin A, we examined the effects of the wild-type and mutant miR-9 expression vectors on two predicted miR-9 target genes, *RBMS3* and *RBM9*, which are thought to encode RNA-binding proteins (20, 21). The wild-type miR-9 expression vector significantly reduced *RBMS3* transcripts; no such effect was detected in cells transfected with the mutant miR-9 vector (Fig. S9*B*). The effects of miR-9 on *RBM9* expression were more modest (Fig. S9*B*). Given that RBMS3 and RBM9 are thought to be RNA-binding proteins, one conceivably could hypothesize that miR-9–mediated changes in RBMS3 or RBM9 might influence changes in prelamin A expression. However, when we knocked down expression of those genes with siRNAs, no effects on prelamin A expression were detected (Fig. S9*C*).

The miR-9 overexpression studies, along with the antisense knockdown experiments, suggested that miR-9 plays a role in regulating lamin A expression in the brain. To explore this issue further, we assessed lamin A expression in the forebrain and cerebellum of both forebrain-specific *Dicer*-knockout mice (*Emx1-Cre* $Dicer^{fl/fl}$) and control mice (*Emx1-Cre* $Dicer^{fl/+}$) (22, 23). The forebrain-specific *Dicer*-knockout mice lack the capacity to produce microRNAs in the forebrain; hence, we suspected that these mice might have higher levels of lamin A in the forebrain (but not in the cerebellum, where *Dicer* expression is preserved). Indeed, as judged by Western blots, lamin A expression was significantly higher in the forebrain of forebrain-specific *Dicer*-knockout mice, but expression in the cerebellum remained low (Fig. S10*A*). Similar results were observed in immunohistochemistry experiments (Fig. S10*B*).

Discussion

The two splice isoforms of the *LMNA* gene, lamins A and C, are major components of the nuclear lamina and are found in roughly similar amounts in cultured fibroblasts and a variety of tissues, including heart, liver, and kidney (4, 11, 12). In the current study, we show that the situation is quite different in the mouse brain. The levels of lamin A in the cerebral cortex and cerebellum are far lower than those in other tissues, as judged by both Western blots and immunohistochemistry. The only cells in the brain that express significant amounts of lamin A are vascular cells and the cells lining the surface of the brain. We observed similar findings in $Zmpste24^{-/-}$ mice (14), which lack the zinc metalloprotease that converts farnesyl-prelamin A to mature lamin A. In those mice, prelamin A is found in the brain, but it is confined to vascular and meningeal cells. Also, only trace

amounts of progerin are found in the cerebral cortex and cerebellum of progerin-only knockin mice (a mouse model of HGPS) (12). Farnesylated prelamin A (in *Zmpste24*$^{-/-}$ mice) and progerin (in the case of HGPS knockin mice) are toxic proteins that elicit multisystem disease phenotypes, but the central nervous system is spared. A plausible explanation for the absence of brain pathology is that the synthesis of the toxic prelamin A proteins is very low in the brain.

RNA studies supported the Western blot and immunohistochemistry findings; Northern blots revealed a low ratio of prelamin A to lamin C transcripts in the cerebral cortex and cerebellum, and those results were confirmed by qRT-PCR studies. We went on to show that the low levels of prelamin A in the brain are caused, at least in part, by removal of prelamin A transcripts by miR-9, a brain-specific microRNA. Multiple lines of evidence support this conclusion. First, transfection of HeLa cells with an miR-9 expression vector lowered lamin A expression levels, as judged by Western blots and immunocytochemistry. Also, when wild-type and *Lmna*$^{HG/+}$ mouse fibroblasts were transduced with lentiviruses encoding miR-9, the levels of lamin A and progerin proteins in the cells fell significantly. Third, expression of miR-9 in HeLa cells reduced prelamin A transcript levels but had no significant effects on transcript levels of lamin C, lamin B1, or lamin B2. A mutant miR-9 expression vector containing a mutation in the seed-binding site had no effect on the expression of prelamin A. Fourth, an antisense oligonucleotide against miR-9 increased prelamin A transcript levels in differentiated neural progenitor cells. In subsequent studies, we identified site 1 (Fig. 6*A*) as the relevant miR-9–binding site in the prelamin A 3′ UTR. Mutation of that site eliminated the capacity of miR-9 to down-regulate the expression of luciferase reporters containing the prelamin A 3′ UTR. As expected, the mutant miR-9 expression vector did not affect the expression of the luciferase-prelamin A 3′ UTR constructs. The microRNA databases have identified a potential miR-129–binding site in the prelamin A 3′ UTR, but we never observed a consistent effect of miR-129 on prelamin A transcript levels or lamin A protein levels in cells.

In overexpression studies, miR-9 reduced prelamin A transcript levels and lamin A protein levels by ∼50%. It is noteworthy, however, that the levels of miR-9 expression that we achieved in transfected cells were only ∼10% of the levels in the cortex of mouse brains. Had we achieved more physiological levels of miR-9 expression, it is conceivable that we would have observed an even greater reduction of prelamin A/lamin A expression in the transfected cells. In contrast, the levels of miR-129 expression in transfected cells were far greater than those in mouse cortex.

The low levels of prelamin A transcripts and lamin A protein in the brain of *Lmna*$^{LAO/LAO}$ mice were pivotal in leading us to consider the potential role of microRNAs in regulating prelamin A expression. In *Lmna*$^{LAO/LAO}$ mice, all the output of the *Lmna* gene is channeled into prelamin A transcripts. Had mRNA splicing been responsible for the low levels of lamin A expression in wild-type brains, we would have observed increased levels of lamin A in the brain of *Lmna*$^{LAO/LAO}$ mice, comparable to levels in other tissues. However, prelamin A transcript levels in *Lmna*$^{LAO/LAO}$ brains were quite low, as were levels of lamin A protein, providing a strong argument against a role for alternative splicing in limiting prelamin A/lamin A expression in the brain. Also, low progerin levels in the brain of progerin-only mice (in which all the output of the gene is channeled into mutant prelamin A transcripts) further supported this conclusion.

The miR-9 overexpression studies, along with the luciferase reporter studies, supported the idea that miR-9 binds to the prelamin A 3′ UTR and down-regulates prelamin A expression in the brain. However, we cannot exclude the possibility that other mechanisms act in an accessory fashion to reduce lamin A expression in the brain. We considered low transcription rates as a contributing factor in the low levels of prelamin A expression in the brain. Arguing against this possibility, however, was the fact that prelamin A hnRNA levels were higher in the brain than in the liver. We also considered the possibility that a distinct promoter for *Lmna* in the brain somehow might underlie the low levels of prelamin A expression in the brain, but the 5′-RACE studies uncovered no evidence that this was the case.

Although our cell-culture experiments strongly supported the idea that miR-9 plays an important role in regulating lamin A expression in the mouse brain, in vivo studies ultimately will be important for better defining the relationship between miR-9 and prelamin A expression in the brain. As a first step, we assessed lamin A expression in forebrain-specific *Dicer*-knockout mice (which lack the ability to produce microRNAs in the forebrain) (22, 23). Interestingly, lamin A levels were higher in the forebrain of these mice, but the levels of lamin A in the cerebellum remained low.

These studies with *Dicer*-knockout mice obviously are consistent with the notion that miR-9 regulates lamin A expression in the brain, but we would emphasize that interpretation of these studies is not straightforward, given that *Dicer* eliminates all microRNAs, and not just miR-9; thus indirect effects on gene expression could occur. In the future, it would be interesting to create and examine miR-9–knockout and overexpression models to assess the effect of miR-9 on lamin A expression, but, again, there likely will be caveats in the interpretation of those experiments, given that miR-9 has other targets as well as prelamin A.

The only cells in the brain of wild-type mice that expressed large amounts of lamin A were vascular and meningeal cells; very little lamin A was observed in neurons or glia. The latter findings are consistent with the fact that both neurons and glia express high levels of miR-9 (24–26). However, many subtleties in the regulation of prelamin A expression by miR-9 still need to be defined. For example, whether there is a simple inverse relationship between miR-9 levels and prelamin A expression in different cell types within the brain—or in different regions of the brain—is not known. Also, the temporal pattern of miR-9 expression in different cell types of the brain is not clear. Thus far, nearly all our studies have been performed on mice that were <5 mo of age, and it is unclear whether miR-9 expression—and the preferential expression of lamin C in the brain—persists in older mice. Even less is known about prelamin A regulation in other species. The patterns of lamin A and lamin C expression in the human brain, for instance, have not been explored at different developmental stages. Furthermore, even though the miR-9–binding site in the prelamin A 3′ UTR is conserved in humans, we do not know if its functional significance is conserved also. In any case, we were intrigued by recent studies of lamin A/C expression in induced pluripotent stem cells generated from human HGPS fibroblasts (27). Upon differentiation into mesenchymal stem cells, lamin A and progerin were expressed highly, but when the same cells were differentiated into neural progenitors, lamin C was the predominant isoform, and the levels of lamin A and progerin were low (27).

The fact that lamin C is expressed highly in the brain implies that it may play an important role in that tissue, but the mouse clearly has evolved a strategy to limit the production of lamin A. Why such a strategy exists is unknown, but one possibility is that the precursor to lamin A, farnesyl-prelamin A, interferes with lamin B1 and lamin B2, both of which are farnesylated proteins with critical functions in the brain. In recent studies, Coffinier et al. (28, 29) have shown that the B-type lamins are crucial for neuronal migration and neuronal viability in the brain. It is conceivable that farnesyl-prelamin A—if produced at high levels in the brain—might compete with the B-type lamins for binding sites along the inner nuclear membrane, whereas lamin C would not. In the future, this concept, along with the physiologic importance of limiting lamin A synthesis in the brain, could be

tested by creating genetically modified mice that produce exclusively prelamin A, rather than lamin C, in the brain.

Aside from providing a window into nuclear lamin biology, the current studies might point to possible strategies for disease therapeutics. The brain makes little prelamin A/lamin A and is spared from the toxicity of mutant forms of prelamin A (e.g., progerin). What the brain achieves with a microRNA could be useful for other tissues. Several years ago, Fong et al. (19) suggested that it might be possible to treat prelamin A-related progeroid syndromes with antisense oligonucleotides against the prelamin A 3′ UTR. Given the current findings, this strategy deserves renewed scrutiny.

Materials and Methods

Mutant Mice. *Zmpste24*$^{-/-}$ mice have been described previously (14). *Lmna*$^{LAO/LAO}$ mice produce exclusively mutant prelamin A transcripts that yield mature lamin A (bypassing prelamin A synthesis and processing) (18). The production of mature lamin A from the *Lmna*^{LAO} transcript, rather than from prelamin A, results from a deletion of the sequences encoding the last 18 amino acids of prelamin A (18). No lamin C is produced by the *Lmna*^{LAO} allele because of the deletion of intron 10 (18). The 3′ UTR in the *Lmna*^{LAO} allele is identical to that of the wild-type allele. We also used *Lmna*$^{nHG/nHG}$ mice, which yield exclusively nonfarnesylated progerin from mutant prelamin A transcripts. The *Lmna*^{nHG} allele has a deletion of introns 10 and 11 along with the last 150 bp of exon 11; it also contains a cysteine-to-serine substitution in the prelamin A *CaaX* motif (12). The 3′ UTR in the *Lmna*^{nHG} allele also retains the wild-type prelamin A 3′ UTR. We used *Lmna*$^{nHG/nHG}$ mice rather than otherwise identical knockin mice expressing farnesylated progerin (10) because *Lmna*$^{nHG/nHG}$ mice survive to adulthood. Finally, we examined forebrain-specific *Dicer*-knockout mice (*Emx1-Cre Dicer*$^{fl/fl}$) and control mice (*Emx1-Cre Dicer*$^{fl/+}$) (22, 23).

Western Blots. Snap-frozen mouse tissues were ground with a mortar and pestle, resuspended in PBS containing 1 mM PMSF, 1 mM NaF, and protease inhibitors (Roche), and then homogenized with a tissue grinder. Protein extracts from HeLa cells and immortalized MEFs were prepared by lysing cells in urea buffer (30, 31). Protein extracts were size-fractionated on 4–12% gradient polyacrylamide Bis-Tris gels (Invitrogen) and then transferred to nitrocellulose membrane. Primary antibodies were a goat polyclonal antibody against lamin A/C (1:400) (sc6215; Santa Cruz); a rat monoclonal antibody against prelamin A (32) (final concentration, 2.5 μg/mL); a mouse monoclonal antibody against lamin B2 (1:400) (33-2100; Invitrogen); a goat polyclonal antibody against actin (1:1,000) (sc1616; Santa Cruz); and a mouse monoclonal antibody against β3 tubulin (TUJ-1) (1:1,000) (sc-58888; Santa Cruz). Antibody binding was detected with IR-Dye–conjugated secondary antibodies (Rockland) and an Odyssey infrared scanner (LI-COR).

Immunofluorescence Microscopy. Mouse tissues were embedded in Optimum Cutting Temperature compound, cryosectioned (10 μm), fixed in methanol, rinsed with acetone, permeabilized with 0.1% (vol/vol) Triton X-100 in Tris-buffered saline, and preincubated with PBS containing 1 mM $CaCl_2$, 1 mM $MgCl_2$, 10% (vol/vol) FBS, and 0.2% (wt/vol) BSA. For cultured cells (HeLa cells and neural progenitor cells), the cells were grown on coverslips, washed with PBS containing 1 mM $CaCl_2$ and 1 mM $MgCl_2$, fixed in methanol, rinsed with acetone, and permeabilized with 0.1% (vol/vol) Triton X-100 in PBS containing 1 mM $CaCl_2$ and 1 mM $MgCl_2$. The following primary antibodies were used: a rat monoclonal antibody against prelamin A (final concentration, 6 μg/mL) (32); a rabbit polyclonal antibody against lamin C (1:200) (LS-B2972; Lifespan Biosciences); a rabbit monoclonal antibody against lamin A/C (1:100) (2921-1; Epitomics); a mouse monoclonal antibody against mature lamin A (1:400) (MAB3540; Millipore); a goat polyclonal antibody against lamin B1 (1:250) (sc6217; Santa Cruz); a hamster monoclonal antibody against CD31 (1:200) (MAB1398Z; Millipore); a rabbit polyclonal antibody against GFAP (1:100) (18-0063; Zymed); a rabbit polyclonal antibody against Olig2 (1:500) (AB9610; Millipore); a rabbit polyclonal antibody against Zic2 (1:200) (AB15392; Millipore); a mouse monoclonal antibody against NeuN (1:500) (MAB377; Millipore); and a mouse monoclonal antibody against β3 tubulin (TU-20) (1:4,000) (ab7751; Abcam). Binding of secondary antibodies was detected with Alexa Fluor 488/568/647-labeled donkey/goat antibodies against rabbit, rat, mouse, or hamster IgG (Invitrogen). After washing and postfixation, DNA was stained with DAPI to visualize nuclei. In some experiments, sections were incubated with an Alexa Fluor 488/555-conjugated anti-lamin A antibody (1:400) (MAB3540; Millipore); an Alexa Fluor 647-conjugated anti-lamin B1 antibody (1:250) (sc6217; Santa Cruz); and an Alexa Fluor 555-conjugated anti-lamin B2 antibody (1:250) (33-2100; Invitrogen). To stain blood vessels, FITC-labeled tomato lectin (Vector Laboratories) was injected i.v. into mice as described (17). Epifluorescence microscopy images were obtained with an Axiovert 200MOT microscope equipped with an ApoTome, and processed with Axiovert 4.6 software (all from Zeiss). Confocal fluorescence microscopy was performed with a Zeiss LSM700 laser-scanning microscope. Images along the *z* axis were captured sequentially, and merged images were generated using Zen 2010 software (Zeiss). To quantify the fluorescence signals, Volocity 3D rendering software (version 5.4; PerkinElmer Improvision) was used to identify nuclei in each image and to measure fluorescence signals from each nucleus.

RNA Studies. Snap-frozen mouse tissues were homogenized in TRI reagent (Molecular Research Center), and total RNA was extracted according to the manufacturer's protocol. RNA (15 μg) was size-fractionated on a 1% (wt/vol) agarose/formaldehyde gel and transferred to a Nytran SuPerCharge nylon membrane (Schleicher and Schuell). The membrane was hybridized with a [^{32}P]dCTP-labeled *Lmna* cDNA probe containing exon 1–4 sequences (shared by prelamin A and lamin C transcripts). A ^{32}P-labeled 18S cDNA probe was used as a loading control. Signals were detected by autoradiography (CL-XPosure Film; Pierce) and quantified by ImageJ software.

Levels of total *Lmna* transcripts, along with levels of prelamin A, lamin C, lamin B1, and lamin B2 transcripts, were assessed by qRT-PCR. For cultured cells (HeLa cells and neural progenitor cells), total RNA was isolated with an RNeasy kit (Qiagen). After DNase I (Ambion) treatment, RNA was reverse transcribed with random primers, oligo(dT) and SuperScript III (Invitrogen). qPCR reactions were prepared with SYBR Green PCR Master Mix (Bioline) and performed on a 7900 Fast Real-Time PCR system (Applied Biosystems). Transcript levels were determined by the comparative cycle threshold method and normalized to levels of cyclophilin A. All primers used are listed in Table S1.

Overexpression of MicroRNAs. HeLa cells were transfected with lentiviral microRNA expression vectors (GeneCopoeia) with FugeneHD (Roche). One day later, transfected cells were subjected to selection with puromycin (final concentration, 5–10 mg/mL) for 2–3 d. For immunocytochemistry studies, no puromycin was added to the cells so that the slides would contain non-transfected control cells. Immortalized MEFs were transduced with lentiviruses encoding miR-9 or miR-129 [generated by the University of California, Los Angeles Vector Core facility from lentiviral microRNA expression vectors (GeneCopoeia)]. Transduced MEFs were subjected to selection with puromycin (final concentration, 5 mg/mL).

MicroRNA levels were assessed by qRT-PCR. Total RNA was isolated with an RNeasy kit (Qiagen), treated with DNase I (Ambion), and reverse transcribed with the miRCURY LNA Universal cDNA synthesis kit (Exiqon). qPCR reactions were prepared with SYBR Green PCR Master Mix and LNA PCR primers (all from Exiqon), and performed on a 7900 Fast Real-Time PCR system (Applied Biosystems). Transcript levels were determined by the comparative cycle threshold method and normalized to levels of U6 snRNA.

Knockdown of miR-9 in Differentiated NPCs. NPCs were isolated from the cerebral cortex of mouse embryos at eE13.5 (33). Cells were plated on poly-L-lysine–coated six-well plates (~8×10^5 cells per well) and cultured in differentiation medium (1:1 mixture of DMEM/F12 and Neurobasal medium supplemented with N2, B27, and penicillin/streptomycin) (33). After 13 d, NPCs were transfected, using FugeneHD (Roche), with an miR-9 antisense oligonucleotide (miRCURY LNA microRNA Power inhibitor against miR-9) or a control antisense oligonucleotide (both from Exiqon). After 7 d, RNA was isolated with an RNeasy kit (Qiagen) and analyzed by qRT-PCR as described earlier.

Luciferase Reporter Assay. The full-length prelamin A 3′ UTR, mutant versions of the prelamin A 3′ UTR, or the lamin C 3′ UTR were cloned downstream of a firefly luciferase gene in pmirGLO (Promega), which contains a Renilla luciferase gene for normalization of the firefly luciferase signal. HeLa cells were transfected with the luciferase reporter vectors along with an empty vector or an miR-9 expression vector (34). In some experiments, we tested the effect of a mutant version of the miR-9 expression vector in which the TTG in the miR-9 seed sequence (CTTTGG) was replaced by GGT. After 24–30 h, cell lysates were analyzed for firefly- and Renilla-luciferase activities with a GloMax luminometer (Promega).

ACKNOWLEDGMENTS. We thank Dr. Douglas Black (University of California, Los Angeles; UCLA) for helpful discussions and Sandy Chang, Yiping Tu, and Chika Nobumori for technical assistance. Lentiviruses were prepared by the UCLA Vector Core facility, which is supported by Jonsson Comprehensive

Cancer Center/P30 CA016042 and CURE: Digestive Diseases Research Center/P30 DK041301. This work was supported by National Institutes of Health Grants HL86683 (to L.G.F.), HL089781 (to L.G.F.), AG035626 (to S.G.Y.), DA017627 (to S.J.P.), and MH083680 (to T.S.), by the Ellison Medical Foundation (T.S.) and the Ellison Medical Foundation Senior Scholar Program (S.G.Y.); by a postdoctoral fellowship award from the American Heart Association, Western States Affiliate (to B.S.J.D.); and by Scientist Development Grants from the American Heart Association (to C.C. and A.P.B).

1. Dauer WT, Worman HJ (2009) The nuclear envelope as a signaling node in development and disease. *Dev Cell* 17:626–638.
2. Schirmer EC, Foisner R (2007) Proteins that associate with lamins: Many faces, many functions. *Exp Cell Res* 313:2167–2179.
3. Dechat T, et al. (2008) Nuclear lamins: Major factors in the structural organization and function of the nucleus and chromatin. *Genes Dev* 22:832–853.
4. Lin F, Worman HJ (1993) Structural organization of the human gene encoding nuclear lamin A and nuclear lamin C. *J Biol Chem* 268:16321–16326.
5. Worman HJ, Fong LG, Muchir A, Young SG (2009) Laminopathies and the long strange trip from basic cell biology to therapy. *J Clin Invest* 119:1825–1836.
6. Davies BS, Fong LG, Yang SH, Coffinier C, Young SG (2009) The posttranslational processing of prelamin A and disease. *Annu Rev Genomics Hum Genet* 10:153–174.
7. Eriksson M, et al. (2003) Recurrent de novo point mutations in lamin A cause Hutchinson-Gilford progeria syndrome. *Nature* 423:293–298.
8. De Sandre-Giovannoli A, et al. (2003) Lamin a truncation in Hutchinson-Gilford progeria. *Science* 300:2055.
9. Hennekam RC (2006) Hutchinson-Gilford progeria syndrome: Review of the phenotype. *Am J Med Genet A* 140:2603–2624.
10. Yang SH, et al. (2005) Blocking protein farnesyltransferase improves nuclear blebbing in mouse fibroblasts with a targeted Hutchinson-Gilford progeria syndrome mutation. *Proc Natl Acad Sci USA* 102:10291–10296.
11. Worman HJ, Lazaridis I, Georgatos SD (1988) Nuclear lamina heterogeneity in mammalian cells. Differential expression of the major lamins and variations in lamin B phosphorylation. *J Biol Chem* 263:12135–12141.
12. Yang SH, Andres DA, Spielmann HP, Young SG, Fong LG (2008) Progerin elicits disease phenotypes of progeria in mice whether or not it is farnesylated. *J Clin Invest* 118: 3291–3300.
13. Sullivan T, et al. (1999) Loss of A-type lamin expression compromises nuclear envelope integrity leading to muscular dystrophy. *J Cell Biol* 147:913–920.
14. Leung GK, et al. (2001) Biochemical studies of *Zmpste24*-deficient mice. *J Biol Chem* 276:29051–29058.
15. Bergo MO, et al. (2002) *Zmpste24* deficiency in mice causes spontaneous bone fractures, muscle weakness, and a prelamin A processing defect. *Proc Natl Acad Sci USA* 99:13049–13054.
16. Young SG, Meta M, Yang SH, Fong LG (2006) Prelamin A farnesylation and progeroid syndromes. *J Biol Chem* 281:39741–39745.
17. Davies BSJ, et al. (2010) GPIHBP1 is responsible for the entry of lipoprotein lipase into capillaries. *Cell Metab* 12:42–52.
18. Coffinier C, et al. (2010) Direct synthesis of lamin A, bypassing prelamin a processing, causes misshapen nuclei in fibroblasts but no detectable pathology in mice. *J Biol Chem* 285:20818–20826.
19. Fong LG, et al. (2006) Prelamin A and lamin A appear to be dispensable in the nuclear lamina. *J Clin Invest* 116:743–752.
20. Fritz D, Stefanovic B (2007) RNA-binding protein RBMS3 is expressed in activated hepatic stellate cells and liver fibrosis and increases expression of transcription factor Prx1. *J Mol Biol* 371:585–595.
21. Yeo GW, et al. (2009) An RNA code for the FOX2 splicing regulator revealed by mapping RNA-protein interactions in stem cells. *Nat Struct Mol Biol* 16:130–137.
22. Murchison EP, Partridge JF, Tam OH, Cheloufi S, Hannon GJ (2005) Characterization of Dicer-deficient murine embryonic stem cells. *Proc Natl Acad Sci USA* 102:12135–12140.
23. Kawase-Koga Y, Otaegi G, Sun T (2009) Different timings of Dicer deletion affect neurogenesis and gliogenesis in the developing mouse central nervous system. *Dev Dyn* 238:2800–2812.
24. Deo M, Yu JY, Chung KH, Tippens M, Turner DL (2006) Detection of mammalian microRNA expression by in situ hybridization with RNA oligonucleotides. *Dev Dyn* 235:2538–2548.
25. Smirnova L, et al. (2005) Regulation of miRNA expression during neural cell specification. *Eur J Neurosci* 21:1469–1477.
26. Lau P, et al. (2008) Identification of dynamically regulated microRNA and mRNA networks in developing oligodendrocytes. *J Neurosci* 28:11720–11730.
27. Zhang J, et al. (2011) A human iPSC model of Hutchinson Gilford Progeria reveals vascular smooth muscle and mesenchymal stem cell defects. *Cell Stem Cell* 8:31–45.
28. Coffinier C, et al. (2010) Abnormal development of the cerebral cortex and cerebellum in the setting of lamin B2 deficiency. *Proc Natl Acad Sci USA* 107:5076–5081.
29. Coffinier C, et al. (2011) Deficiencies in lamin B1 and lamin B2 cause neurodevelopmental defects and distinct nuclear shape abnormalities in neurons. *Mol Biol Cell* 22:4683–4693.
30. Fong LG, et al. (2004) Heterozygosity for Lmna deficiency eliminates the progeria-like phenotypes in Zmpste24-deficient mice. *Proc Natl Acad Sci USA* 101:18111–18116.
31. Steinert P, Zackroff R, Aynardi-Whitman M, Goldman RD (1982) Isolation and characterization of intermediate filaments. *Methods Cell Biol* 24:399–419.
32. Lee R, et al. (2010) Genetic studies on the functional relevance of the protein prenyltransferases in skin keratinocytes. *Hum Mol Genet* 19:1603–1617.
33. Ader M, Meng J, Schachner M, Bartsch U (2000) Formation of myelin after transplantation of neural precursor cells into the retina of young postnatal mice. *Glia* 30: 301–310.
34. Delaloy C, et al. (2010) MicroRNA-9 coordinates proliferation and migration of human embryonic stem cell-derived neural progenitors. *Cell Stem Cell* 6:323–335.